A Journal of the Gesellschaft Deutscher Chemiker

Angewandte International Edition GDCh Chemie

www.angewandte.org

Accepted Article

Title: Supercharging prions via amyloid-selective lysine acetylation

Authors: Katelyn M. Baumer, Christopher D. Cook, Collin T. Zahler, Alexandra A. Beard, Zhijuan Chen, Jordan C. Koone, Chad M. Dashnaw, Raul A. Villacob, Touradj Solouki, John L. Wood, David R. Borchelt, and Bryan F. Shaw

To be cited as: *Angew. Chem. Int. Ed.* 10.1002/anie.202103548

Link to VoR: https://doi.org/10.1002/anie.202103548

WILEY-VCH

10.1002/anie.202103548

Supercharging prions via amyloid-selective lysine acetylation

Running title: Supercharging amyloid

Katelyn M. Baumer[a], Christopher D. Cook[a], Collin T. Zahler[a], Alexandra A. Beard[a], Zhijuan Chen[b], Jordan C. Koone[a], Chad M. Dashnaw[a], Raul A. Villacob[a], Touradj Solouki[a], John L. Wood[a], David R. Borchelt[b], Bryan F. Shaw[a*]

[a]Department of Chemistry and Biochemistry, Baylor University, Waco, TX

[b]Department of Neuroscience, University of Florida, Gainesville, FL

*To whom correspondence should be addressed: bryan_shaw@baylor.edu

Keywords: superoxide dismutase, neurodegeneration, amyotrophic lateral sclerosis, protein aggregation, acetylation.

10.1002/anie.202103548

Abstract

Repulsive electrostatic forces between prion-like proteins are a barrier against aggregation. In neuropharmacology, however, a prion's net charge (Z) is not a targeted parameter. Compounds that selectively boost prion Z remain unreported. Here, we synthesized compounds that amplified the negative charge of misfolded superoxide dismutase-1 (SOD1) by acetylating lysine-NH_3^+ in amyloid-SOD1, without acetylating native-SOD1. Compounds resembled a "ball and chain" mace: a rigid amyloid-binding "handle" (benzothiazole, stilbene, or styrylpyridine); an aryl ester "ball"; and a triethylene glycol chain connecting ball to handle. At stoichiometric excess, compounds acetylated up to 9 of 11 lysine per misfolded subunit (ΔZ_{fibril} = -8,100 per 10^3 subunits). Acetylated amyloid-SOD1 seeded aggregation more slowly than unacetylated amyloid-SOD1 *in vitro* and organotypic spinal cord (these effects were partially due to compound binding). Compounds exhibited reactivity with other amyloid and non-amyloid proteins (e.g., fibrillar α-synuclein was peracetylated; serum albumin was partially acetylated; carbonic anhydrase was largely unacetylated).

Introduction

Because most proteins carry an intrinsic net electrostatic charge (Z) between Z = +10 and -10 (at cytosolic pH), they exert Coulombic forces upon each other.[1] Debye-Hückel theory predicts that these intermolecular forces—attractive or repulsive per each protein's sign of net charge—reach 10 Å through solvent.[2] In the case of a partially desolvated protein undergoing self-assembly, the Debye length could reach ~ 20-50 Å through its hydrophobic interior, assuming an interior ionic strength of I = 0.001 and a dielectric constant (ε) between 4 and 20.

Despite the central importance of Z in molecular recognition, protein aggregation[3] and catalysis,[4] the net charge of a protein is not typically targeted as a druggable parameter in pharmacology—at least not intentionally. Typically, pharmacons are not designed to function Coulombically, by adjusting long-range electrostatic forces.[5] Rather, most pharmacons are thought to function sterically by inserting hydrophobic or dipole-dipole interactions that alter other classical parameters, including the K_m or V_{max} of an enzyme; ΔG_{fold}; or the K_d of a protein-protein interaction. There are, however, some drugs that have high values of net charge and unclear mechanisms of action (e.g., the century-old drug, suramin[6]). These drugs might function by altering electrostatic interactions.

The central hypothesis of this study is that small molecules can be designed and synthesized to selectively increase the net charge of prion-like amyloid assemblies[7] by magnitudes that inhibit their propagation. The rationale for this hypothesis is based upon: (i) the general negative correlation between the rate of aggregation of proteins and their magnitude of net charge;[8-9] (ii) the occurrence of pathogenic missense mutations that accelerate aggregation of the gene product by diminishing its net charge;[3, 8, 10] and (iii) the use of anhydrides or aryl esters to post-translationally "supercharge"[9] anionic proteins by non-selective hyperacylation of lysine-NH_3^+.[11-12]

To this end, we designed and synthesized compounds to selectively amplify the net negative charge of amyloid fibrils of Cu, Zn superoxide dismutase-1 (SOD1)[13] by amyloid-selective acetylation of lysine-ε-NH_3^+. Misfolded forms of SOD1 (a negatively charged protein[14]) cause amyotrophic lateral sclerosis (ALS) by a prion-like mechanism.[15] Previous studies using "protein charge ladders" and capillary electrophoresis—one of the few methods for measuring the net charge of folded proteins at pH ≠ pI—found that native wild-type (WT) SOD1 retains a small negative charge across subcellular pH and Cu/Zn stoichiometry.[14] For example, the net charge of SOD1 varies from Z = -3.69 to -6.06 per subunit (pH 7.4), depending upon the number of bound Cu^{2+} and Zn^{2+}.[14] The holo-enzyme (with 2 Cu^{2+} and 2 Zn^{2+} per dimer) remains anionic from pH 5 to 8, bearing a minimal net charge of Z = -1.9 per subunit at lysosomal pH.[14] Several ALS-linked mutations in SOD1 located at the protein's surface (e.g., D90A, E100K, N139K, D101N) are thought to promote SOD1 aggregation by reducing the net charge of SOD1.[10, 16-17]

Compounds were designed to accomplish amyloid-selective acylation by linking an aspirin-like aryl ester (that is weakly reactive with lysine) to one of three different hetero- or homocyclic scaffolds that bind amyloid[18-20] (Figure 1). We hypothesized that these amyloidophilic, aspirin-like compounds would bind amyloid fibrils of SOD1 and selectively acetylate its lysine, while being too unreactive to acylate residues in native SOD1 (Figure 1). We chose lysine acylation to supercharge amyloid SOD1 because lysine acylation with non-selective anhydrides or free aspirin inhibits the prion-like propagation of aggregated SOD1 *in vitro* and in organotypic spinal cord.[21-22] Lysine-ε-NH_3^+ groups are also involved in specific short-range interactions between misfolded proteins.[23]

Results & Discussion

Design and synthesis of "ball and chain" molecular maces

Three different compounds were synthesized to contain a nitrated aryl ester tethered to a benzothiazole (BT), stilbene (SB), or styrylpyridine (Py) group via a triethylene glycol linker (Scheme 1). Benzothiazole, stilbene, and styrylpyridine motifs were used as "handles" because derivatives of these species exhibit general binding affinity for amyloid-like fibrils.[18-20] The chemical anatomy and putative function of these amyloidophilic aryl esters is analogous to a medieval "ball and chain" mace: an amyloidophilic "handle"; a reactive aryl ester "ball" that acetylates lysine-ε-NH_3^+; and a flexible triethylene glycol "chain" that permits acetylation of lysine-ε-NH_3^+ within ~12 Å of the handle's binding site (Figure 1). Synthesis of "ball and chain" maces is outlined in Scheme 1. Synthesis of the BT, SB, or Py handles and chain utilized previously published procedures.[19-20, 24] The full synthesis is described in Supporting Information.

The "handles" for all three compounds (and "chains" for stilbene and styrylpyridine derivatives) are similar to three FDA-approved ^{18}F Positron Emission Tomography (PET) agents for imaging amyloid plaques in Alzheimer's disease.[18-20] The length of the glycol chain was chosen to be identical to the glycol chains present in two of these PET agents. A weakly reactive nitrated aryl ester—a derivative of aspirin[22] —was used as the reactive "ball." The mild reactivity of the aryl ester was empirically tuned by conjugation to the glycol and addition of the nitro group (which we found to be required for acetylation of lysine in water). The weak reactivity of the ester is intended to minimize off-target acylation of non-amyloid proteins that do not bind the compound (i.e., increased collision frequency between aryl ester and Lys-ε-NH_3^+ in the amyloid-mace complex will promote acylation, while the free compound will be too unreactive to acylate non-amyloid proteins). The long half-life of amyloid-like complexes *in vivo* will allow, we hypothesize,

for successive binding and acetylation, leading to cumulative acetylation and supercharging of amyloid-like assemblies (Figure 1B).

In this study, metal-free (apo) wild-type SOD1 was generated by demetallation in EDTA, with a final metal content of ≤ 0.08 molar equivalents of Cu^{2+} or Zn^{2+} per dimer (according to ICP-MS). This study targeted wild-type SOD1 because: (i) WT SOD1 promotes the toxicity of ALS-linked mutant SOD1 and is required for pathogenesis in some ALS models (and most ALS-SOD1 mutations are heterozygous);[25-26] and (ii) WT apo-SOD1 forms amyloid fibrils *in vitro* at rates identical to several ALS mutant apo-SOD1 proteins.[27]

Ball and chain molecular maces acetylate fibrillar apo-SOD1 but not native holo-SOD1

Reactivity of the molecular mace compounds with fibrillar apo-SOD1 or native holo-SOD1 was tested by incubating 30 μM SOD1 (60 μM SOD1 monomer) with 3 mM compound in a gyrating microplate for 5 days (37 °C, 3 % DMSO). The effective molar excess of mace per SOD1 monomer is likely lower than 50:1, as compounds are minimally soluble in pure water (similar to their PET analogs) with precipitation observed upon dilution into protein solution. The predicted solubility of mace compounds in pure water (25 °C) ranged from 0.20-0.93 μg/mL; 0.24 to 1.69 μM. Experimentally measured solubility in 97 % H_2O/ 3 % DMSO (37 °C) ranged from 0.18 to 4.6 μM (Figure S1).

The extent of acetylation after incubation was quantified with mass spectrometry (Figure 2) and capillary electrophoresis using UV absorbance at 214 nm (Figures 3, S2). See Supporting Information for a discussion of the use of mass spectrometry and capillary electrophoresis to quantify lysine acetylation. After a five-day incubation, fibrillar SOD1 and native holo-SOD1 were both treated with 1,1,1,3,3,3-hexafluoro-isopropanol (HFIP) (Figure S3). Hexafluoroisopropanol

was used to defibrillize SOD1 (Figure S3) prior to analysis via mass spectrometry or capillary electrophoresis because it effectively quenches acetylation by lowering solvent pH to ~ 3.

Native holo-SOD1 remained unacetylated after incubation with all three molecular maces (Figure 2), however, fibrillar SOD1 was acetylated by each mace. The weighted average number of acetylated lysine residues in fibrillar apo-SOD1 (per subunit) following incubation with BT, SB, or Py is as follows: BT, 2.27 acetylated lysine (20.17 % of SOD1 proteins unacetylated); SB, 1.66 (10.52 % unacetylated); Py, 3.98 (0.00 % unacetylated) (Figure 2). These differences in reactivity between compounds might be caused in part by differences in solubility and/or unique binding sites on fibrils. No clear correlation was found between solubility and reactivity (Figures S1, S4). Note the concentration of acetylated lysine in SOD1 (e.g., [3.98 Lys-Ac] × [60 μM SOD1 monomer], in the Py-treated sample) is much larger than the maximum solubility of the Py compound. Thus, the compound must be partitioning from the colloidal phase to fibrillar SOD1 over the reaction period.

Capillary electrophoresis of acetylated monomers recovered from fibrils demonstrated that lysine acetylation increased net negative charge by ~ -0.9 units, rather than -1 because of charge regulation (Figure 3).[2] Charge regulation refers to the adjustment in pK_a of ionizable residues, in response to the new electrostatic environment caused by acetylation.

Note that the BT-treated fibrils have, relative to SB-treated fibrils, both a higher weighted average number of acetyl modifications *and* a higher percentage of unmodified protein (Figure 2). This paradox is caused by a greater degree of positive skewness in the distribution of acetyl peaks for the BT sample (reaching 8 acetyl modifications) than the SB sample (reaching only 4 acetyl modifications). This positive skewness might suggest cooperativity in acetylation of fibrils by BT (e.g., perhaps acetylation promotes partitioning of compound to fibril).

To determine if maces exhibited high reactivity with other fibrillar proteins, we incubated each mace with fibrillar α-synuclein. Alpha-synuclein has 14 lysine and a formal net charge of Z = -9.0 (the form we used lacked N-terminal acetylation). After a five day incubation with each compound at a ratio of ~ 43:1 (compound:protein), the weighted average number of acetylations is as follows; BT, 10.22; SB, 7.83; Py, 7.11 with no unacetylated protein remaining (Figure S5). Thus, as far as the percent of lysine that were acetylated, maces were most reactive with fibrillar α-synuclein compared to fibrillar SOD1 (or any native protein in this study), doubling the formal net charge up to Z = -18. We did not perform a five day control experiment with native α-synuclein (an intrinsically disordered protein[28]) as it readily fibrillizes.

The exact residues acetylated by the molecular mace compounds were identified via sequential trypsin and pepsin proteolysis and liquid chromatography tandem mass spectrometry ($LC\text{-}MS^E$) (Figure 2, S6, S7). The sequence coverage for each solution of mace-acetylated SOD1 fibrils was 100 % and the identity of acetylated residues was based upon manual inspection of mass spectra and the following threshold criteria: a peptide mass error < 6 ppm; fragment root mean square mass error < 30 ppm; signal to noise ratio > 3.

Tandem mass spectrometry suggested that lysine residues were selectively acetylated over other nucleophilic residues in amyloid-SOD1 (Figure 2, S6). The N-terminus of human SOD1 protein in this study is properly acetylated by the eukaryotic host expression system. A comparison of the MS/MS and MS spectra suggests that each molecular mace does not exhibit selectivity to a single lysine residue in fibrillar SOD1 (Figure 2, S6, S7). All lysine residues were acetylated by each molecular mace with the exception of: (i) Lys 128 when reacted with BT, and (ii) Lys 3 when reacted with SB (Figure 2, S6). Acetylation of multiple lysine in fibrillar SOD1 is presumably permitted by the flexible glycol linker in combination with the multiple binding sites on each

fibril.[29-31] Although we present mass reconstructs of acetylated and unacetylated fragments including each lysine (Figure S6), we reiterate that the intensity of mass spectral signals cannot be used to quantify acetylation because: (i) acetylation of lysine can lower ionization efficiency of small peptides, and (ii) alter proteolysis sites of trypsin or pepsin.

Capillary electrophoresis was used to estimate the electrostatic effects of each compound on fibrillar SOD1 (Figure 3). The capillary electropherograms of defibrillized SOD1 are generally superimposable with the mass spectra in Figure 2. According to the increased mobility of acetylated SOD1, acetylation increased the magnitude of Z of each SOD1 polypeptide from Z = -6.92 for unacetylated apo-SOD1 (previously determined)[14] to between Z = -7.80 and -13.96 for BT (weighted average: Z = -8.92); between Z = -7.86 and -10.68 for SB (weighted average: Z = -8.48); and between Z = -7.87 and -15.47 for Py (weighted average: Z = -10.70) (Figure 3). In a fibril consisting of 10^3 peptides, this amplification of Z is equivalent to ΔZ_{ave} = - 2,400 units/fibril and ΔZ_{max} = -8,100 units/fibril.

Molecular maces were tested for reactivity against other abundant, natively folded proteins including holo-myoglobin (equine heart, 19 lysine), holo-α-hemoglobin (bovine blood, 13 lysine), holo-cytochrome c (equine heart, 19 lysine), α-lactalbumin (bovine, 12 lysine), carbonic anhydrase II (bovine, 18 lysine), ubiquitin (bovine, 6 lysine), and serum albumin (human, 60 lysine). These proteins were chosen because: (i) each does not form amyloid or aggregate under conditions used for fibrillization of apo-SOD1 (Figure S8); (ii) each contains an unacetylated N-terminal α-NH_3^+ (which is generally more reactive with aryl esters than lysine-ε-NH_3^+); (iii) each (except for ubiquitin) contains more lysine than SOD1; and (iv) the net charge of some of these proteins are either net positive or less negative than SOD1, suggesting that their lysine residues have lower pK_a

(and are thus more reactive with aryl esters). Thus, these proteins are good controls for off-target acetylation.

Following incubation in a gyrating microplate (360 rpm; 37 °C) for five days, acetylation of each protein was determined via LC-MS (Figure S9) and verified with capillary electrophoresis (see Supporting Information). The weighted average acetylation of each protein varied between 0.10 acetyl groups for carbonic anhydrase II and 0.14 acetyl groups for cytochrome c and myoglobin, up to 2.69 acetyl groups for hemoglobin (Figure S9).

Serum albumin was the most acetylated native protein that we studied and is a special case. We could not integrate all ions to determine accurate weighted averages of numbers of acetylated lysines because the mass spectra of HSA are reportedly difficult to deconvolute due to persistent impurities.[32] We could, however, calculate the number of acetylated lysine on the most abundant ions. Of the 60 lysine in HSA, we estimate that BT acetylated between 3-34 Lys (median ~ 15 Lys), SB acetylated 1-43 Lys (median ~ 15 Lys), and Py acetylated 12-45 Lys (median ~25 Lys). Unacetylated HSA was not detected. This high degree of acetylation is not particularly surprising considering its high affinity for drug-like molecules including stilbenes and benzthiazoles.[33-34] This result offers more evidence to support the hypothesis that binding of the mace promotes acylation of lysine. The identity of acetylated residues was determined by tandem mass spectrometry (Figure S10, Tables S1-S7), with sequence coverage ranging from 86 to 100 %.

Tandem mass spectrometry suggested that maces react with N-terminal α-NH_3^+ in Mb, CAII, Ubq, and α-Lac however, we did not detect N-terminal acetylation in Cyt c or Hb (detecting N-terminal fragments with LC-MS and MS/MS can be challenging due to their small size). Acetylated lysine residues were detected in all control proteins (Figure S10, Tables S1-S7). We cannot entirely rule out that maces are binding these heme proteins specifically, however, we

suspect that these proteins are more reactive than native holo-SOD1 because each contains an N-terminal α-NH_3^+, more lysine residues than SOD1, and are less anionic/more cationic than SOD1.

In vitro seeding activity of SOD1 parent fibrils acetylated by molecular mace compounds

The ability of supercharged and normally charged apo-SOD1 (formed in the presence of BT, SB, Py, or a DMSO control) to recruit soluble apo-SOD1 into the fibrillar state (i.e., to seed aggregation) was measured with Thioflavin-T (ThT) fluorescence (Figure 4). We examined how acetylation by molecular maces altered the seeded fibrillization of SOD1 (rather than of unseeded fibrillization) for two reasons. First, seeded assays using "parent" fibrils permit us to test how molecular maces affect the prion-like propagation of fibrils in vitro, which can be compared to seeding assays in organotypic mouse spinal cord. Second, the unseeded fibrillization of SOD1 is highly stochastic, with lag times ranging from ~ 5 to > 20 hours for identical solutions of SOD1.[35] Seeded fibrillization of native apo-SOD1 with pre-formed "parent" fibrils (consisting of apo-SOD1) is less stochastic and statistically significant kinetic values can be easily obtained.[36]

The seeded fibrillization of SOD1 with untreated (unacetylated) SOD1 parent fibrils (denoted DMSO control) exhibited exponential increases in ThT fluorescence without a calculable lag time (as expected when by-passing primary nucleation by addition of an amyloid seed[37]). Fitting of data to exponential functions was performed because sigmoidal fits resulted in illogical kinetic parameters, i.e., infinite error for any parameter or initial or maximum fluorescence values that were orders of magnitude above (i.e., 10^4-fold larger) what is observed. Parent fibrils treated (acetylated) with the Py molecular mace compound exhibited a diminished ability to seed the fibrillization of SOD1, as illustrated by an increase in lag time of more than four hours ($p \leq 0.0001$) and two-fold decrease in propagation rate ($p \leq 0.0001$) compared to fibrils grown in the presence

of DMSO treated seeds (Figure 4). Treating fibrils with BT and SB molecular mace compounds resulted in weaker inhibitory effects on seeding compared to Py treated fibrils. Note that while the BT and SB compound did increase lag time compared to the DMSO control ($p \leq 0.0001$) the SB compound did not affect propagation rate compared to the DMSO control ($p = 0.5563$, Figure 4E). These data might be rationalized by the fewer numbers of lysine residues acetylated by BT and SB (Figure 4).

To determine how maces might affect seeding activity of fibrillar SOD1, independent of lysine acetylation, "whip" compounds were synthesized that contained the handle and glycol chain but lacked the reactive nitrated aryl ester (Figure 4). Fibrils that were treated with unreactive "whips" (denoted BTOH, SBOH, PyOH) did not produce increased lag times of fibrillization in assays of seeded fibrillization (Figure 4D). The BTOH and SBOH whips were slightly more effective at inhibiting fibril elongation than their corresponding maces. This effect might be due to the intrinsic inhibitory effects of the handle on elongation, combined with the higher solubility of whips compared to maces (whips are predicted to be 100-fold more soluble in water than maces). It has been shown that high concentrations of amyloid-binding compounds, such as Thioflavin-T, can slow the fibrillization of certain proteins, however, the effects on SOD1 are unknown.[38]

Is acetylation—or more generally, the molecular mace—inhibiting fibrillization by a purely electrostatic mechanism? According to our data, probably not. Previous studies examined how SOD1 fibrillization is affected by acylation with different non-specific anhydrides that attach groups of variable charge, flexibility, and hydrophobicity.[21-22] These studies suggest that the inhibitory effect of lysine acylation on SOD1 fibrillization is largely electrostatic in nature.[21-22] Previous reports analyzed how the acetylation of soluble SOD1 with aspirin affected the nucleation

and elongation of amyloid-like fibrils.[22] These prior experiments involved the free aryl methyl ester (aspirin), unattached to an amyloid-binding moiety, and found that acetylation of ~ 3 lysine per SOD1 subunit increased lag time by 2.6 hours (in unseeded assays); acetylation of ~ 6 lysine increased lag time by 11 hours.[22] Despite these results, we cannot rule out inhibitory effects from increased polydispersity, caused by myriad regioisomeric forms of acetylated SOD1 and from the binding of the compound itself (as demonstrated by control studies with whips).

Control experiments were performed to determine how acetylation of lysine by the free aryl ester "ball" affected the seeding properties of fibrillar SOD1. The free aryl ester acetylated lysine in holo-SOD1, fibrillar apo-SOD1, and in native control proteins (Figure S11). Addition of the free aryl ester to SOD1 produced a weighted average of 6.51 acetyl groups per subunit for fibrillar apo-SOD1 and 7.28 acetyl groups per subunit of native holo-SOD1 (unacetylated protein = 0 % for native and fibrillar SOD1; Figure S11). The increased reactivity of the free "ball" compared to the mace is attributed to the greater intrinsic reactivity of the untethered aryl ester (fewer steric constraints during nucleophilic attack by lysine side chain). The SOD1 fibrils that were acetylated by the free aryl ester exhibited weak seeding activity, with a lag time of 21.9 ± 1.4 hours and a propagation rate of 3.7 ± 0.1 hr^{-1} (Figure 4). These rates are slower than those of seeded fibrillization with unacetylated or mace-acetylated amyloid seeds (Figure 4) and are comparable to rates of unseeded fibrillization.[36] This long lag time suggests that the extensive acetylation by the free ester inhibited the formation of a competent amyloid seed.

Seeding of ALS-linked G85R SOD1 by supercharged SOD1 fibrils in organotypic spinal cord

We compared the prion-like activity of supercharged SOD1 fibrils and unacetylated SOD1 fibrils in organotypic murine spinal cord. The spinal cord cultures were derived from transgenic

mice expressing human ALS-variant SOD1 fused to yellow fluorescent protein (G85R-SOD1:YFP). This transgenic line has been shown to be a valid *ex vivo* assay for prion-like seeding activity of SOD1 amyloid fibrils that are produced exogenously.[39] The expression level of mutant SOD1:YFP in these transgenic animals is too low to produce disease or SOD1:YFP inclusion pathology.[40] Rather, large inclusions of endogenously expressed ALS-mutant SOD1:YFP (micron-scale) are only observed when exogenous SOD1 fibrils are injected into culture media (or when spinal cord extract from a symptomatic ALS-SOD1 Tg mouse is added).[40] Currently, we do not know the mechanism(s) by which exogenously added SOD1 fibrils interact with (and seed aggregation of) endogenously expressed G85R SOD1:YFP in organotypic spinal cord. A prion-like mechanism involving endocytosis of misfolded WT SOD1 is possible.[15]

The prion-like seeding activity of acetylated SOD1 fibrils (produced *in vitro* and treated with molecular mace compounds) was monitored by adding fibrils directly to cultured cross-sectional slabs of G85R-SOD1:YFP spinal cord (Figure 5A-F). As a positive control, seeds from spinal cord homogenate (of an ALS- symptomatic G93A SOD1 mouse) were added to G85R-SOD1:YFP slabs, resulting in extensive inclusion pathology (Figure 5A). Experiments involving mice were approved by the University of Florida Institutional Animal Care and Use Committee (IACUC).

The addition of unacetylated SOD1 fibrils from *in vitro* preparations also produced multiple inclusions (Figure 5C), as previously observed[21] for unacetylated fibrils of WT SOD1. The addition of SOD1 fibrils treated with BT, SB, or Py (identical to those fibrils used to measure *in vitro* seeding activity) had variable effects on *ex vivo* seeding activity in spinal cord (Figures 5D-F, S12A-C). Consistent with *in vitro* seeding data (i.e., effect of compounds on lag time or fibril propagation rate), the most pronounced inhibitory effects on *ex vivo* seeding activity were

observed for fibrils treated with the Py molecular mace, and with BTOH and SBOH whips (Figures 5G-H). Additional replicates and images of spinal cord slices incubated with SOD1 seeds treated with whip compounds can be found in the supporting information (Figure S12).

The addition of spinal cord homogenate from ALS G93A mice (i.e., "control" seeds) produced 285 ± 172 inclusions per cultured spinal cord slab (Figure 5G). Addition of unacetylated fibrillar SOD1 to 12 slabs (labelled "DMSO" in Figure 5) produced 90 ± 48 inclusions. The addition of mace-treated acetylated fibrils resulted in < 50 inclusions per slab (12 slabs), with the Py-treated fibrils producing the lowest value of 23 ± 14 inclusions per slab. The effect of mace-treated fibrils on the formation of inclusions in spinal cord slabs correlated with seeding activity of *in vitro* fibrillization assays (Figure 5H). In both experiments, the Py molecular mace was the most effective at inhibiting aggregation. Note that the Py mace was more effective than the Py whip at inhibiting inclusion formation, whereas the inhibitory effects of other maces were statistically similar to their corresponding whip (Figure 5H, Figure S12). Moreover, the BTOH and SBOH whips were as effective as the Py mace at inhibiting inclusion formation (Figure 5H). These results mirror the comparative effects of whips and maces on fibril elongation rates *in vitro* (Figure 4E, Figure 5H). We hypothesize that BTOH and SBOH whips inhibited inclusion formation (as equally well as the Py compound) due to their possible inhibitory effects on fibril elongation[38] and 100-fold greater solubility (predicted) compared to mace compounds.

Cytotoxicity of Molecular Maces

The intrinsic cytotoxicity of each molecular mace and the free aryl ester "ball" were estimated via an MTT (3-[4,5-dimethylthiazole-2-yl]-2,5-diphenyltetrazolium bromide) viability assay using CHO-K1 cells (ATCC CCL-61). Cells were incubated with each compound at

concentrations ranging from 0.1 to 100 μM in 5% DMSO. No decrease in cell viability was observed. (Figure S13). A caveat of this result is that compounds are only immediately soluble up to ~ 4 μM (Figure S13). The free aryl ester "ball" is, however, highly soluble and did not lead to a decrease in cell viability up to 100 μM.

"Drugging Z"

The "ball and chain" molecular maces described in this study represent, to our knowledge, the first example of compounds that selectively modify a protein (covalently) in its amyloid-like state, without reacting with lysine in the native state of the same protein. The potential utility of molecular maces as lead compounds, and their shortcomings, are discussed in Supporting Information. While this proof of concept study designed molecular maces to transfer one of the simplest and least potent (in terms of Δ*Z*) types of acyl groups (R-C=OCH_3), this strategy is not limited to acetylation. Future ball and chain maces can include non-biological acyl groups that impart more than a single unit of charge (and are not substrates for de-acylation[41]). This study suggests that any useful "supercharging" compound would require a more electrostatically potent group than acetyl, as acetylation did not greatly reduce aggregation in all cases, compared to the corresponding whip. The molecular mace compounds described in this study also provide a means of covalently attaching probes (including ^{13}C and ^{18}O) to lysine residues in amyloid-like species for *in vivo* tracking, imaging[42] or proteomic analysis. The structural similarity between "ball and chain" molecular maces and FDA approved PET agents for amyloid plaques of $A\beta_{1-42}$ also suggests that molecular maces will be capable of supercharging other misfolded prion-like proteins besides SOD1 and α-synuclein.[43]

Acknowledgement

We would like to thank the Mass Spectrometry Center, Molecular Bioscience Center, and the Center for Microscopy and Imaging at Baylor University for use of facilities and instrumentation.

Funding

This research was supported by grants from the National Science Foundation (CHE: 1856449, CHE: 1352122), the Welch Foundation (AA-1854), and the National Institutes of Health (1R01NS092788).

10.1002/anie.202103548

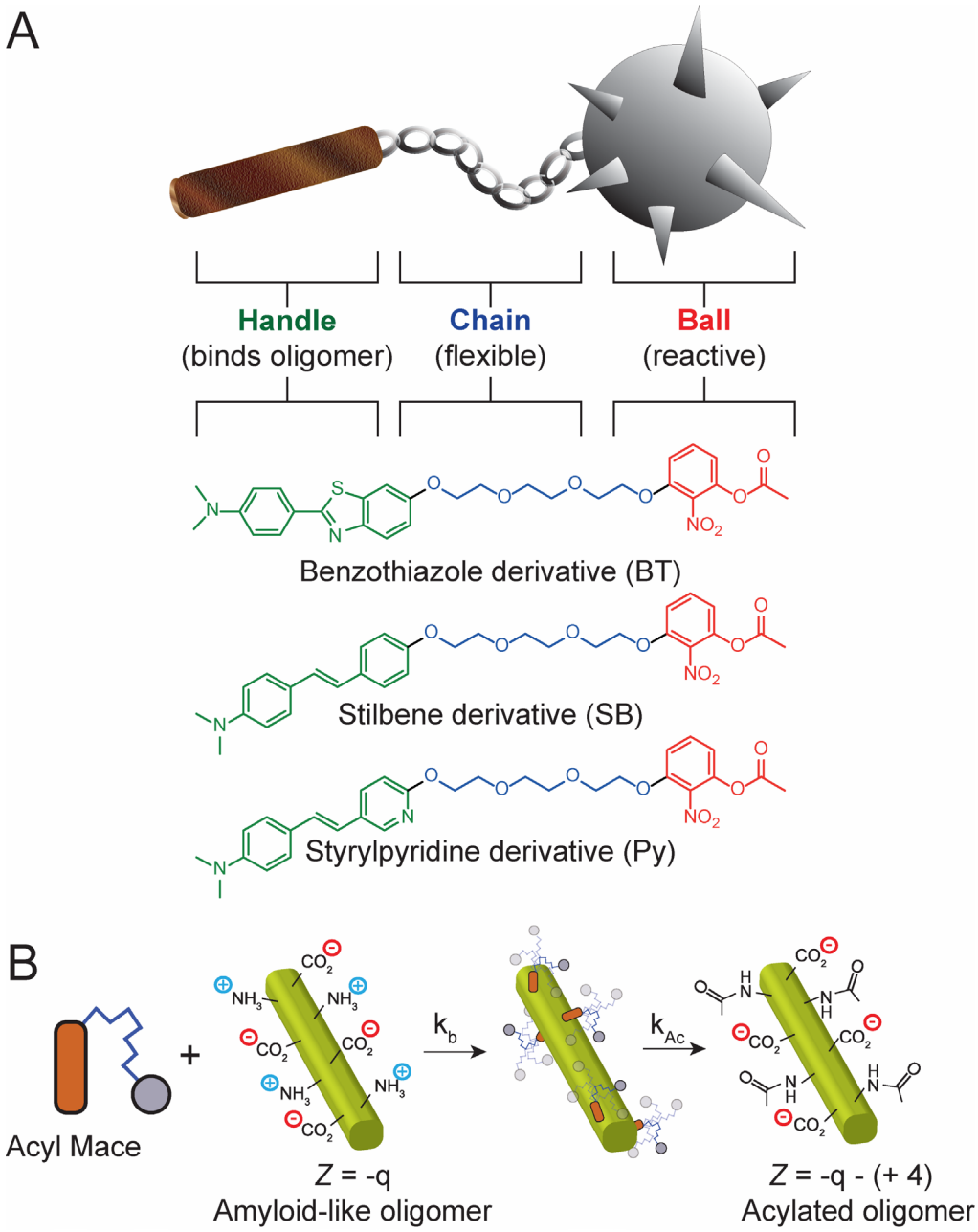

Figure 1. Amplifying the net charge (Z) of misfolded SOD1 by amyloid-selective lysine acetylation. (A) Structures of the three "ball and chain" molecular mace compounds synthesized in this paper. (B) Acetylation (neutralization) of Lys-ε-NH_3^+ will increase the magnitude of net negative charge of amyloid-like assemblies. In this illustration, the rate of acylation (k_{Ac}) is slower than the rate of binding (k_b).

10.1002/anie.202103548

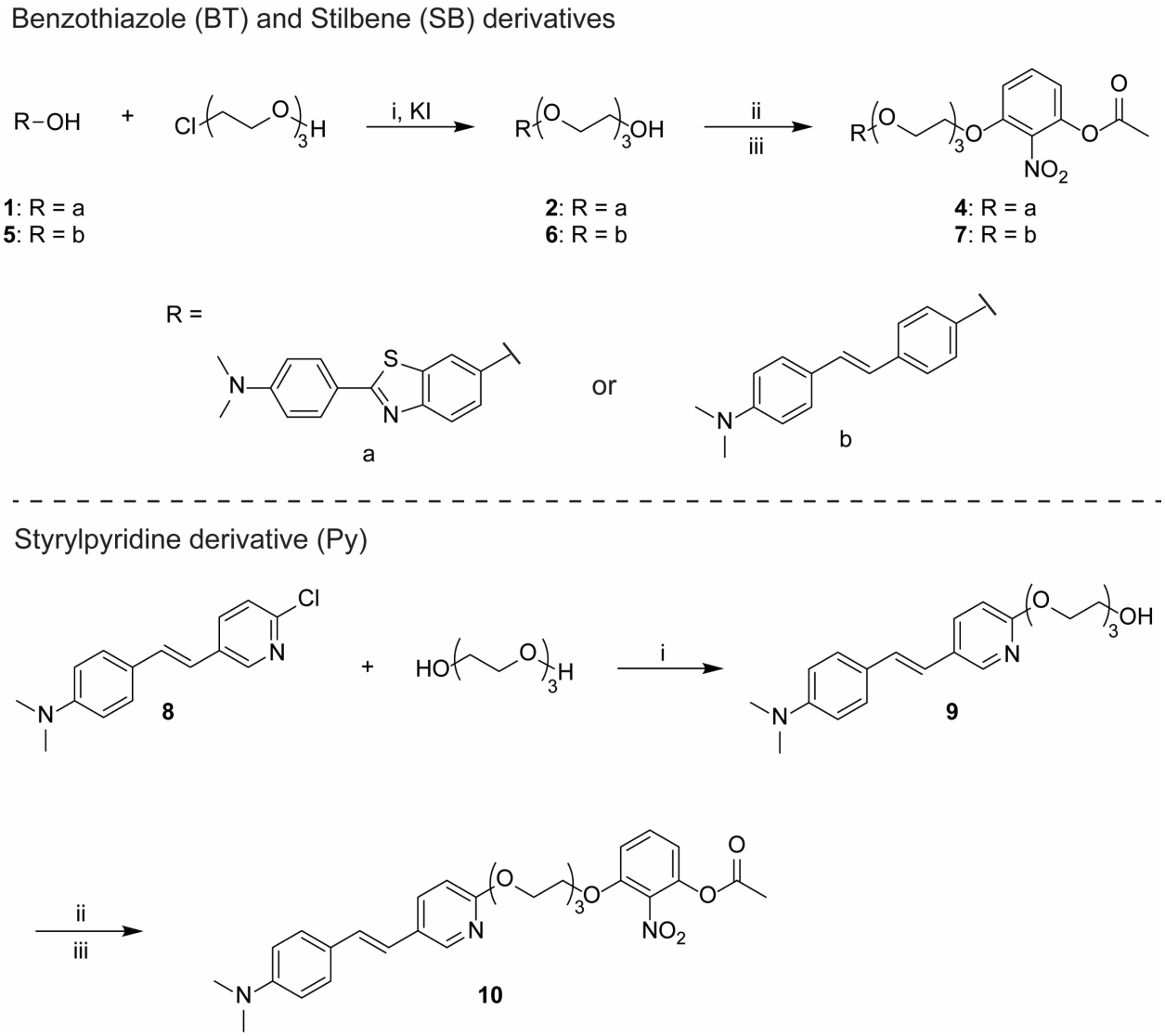

Scheme 1. Synthesis of BT, SB, and Py molecular maces. *Reagents and conditions:* (i) K_2CO_3, DMF, 180 °C, 16 hours (ii) 2-nitroresorcinol, PPh_3, DIAD, THF, 24 hours (iii) Et_3N, AcCl, DCM, ~ 12 hours. See supplementary note for ^1H and ^{13}C NMR spectra.

10.1002/anie.202103548

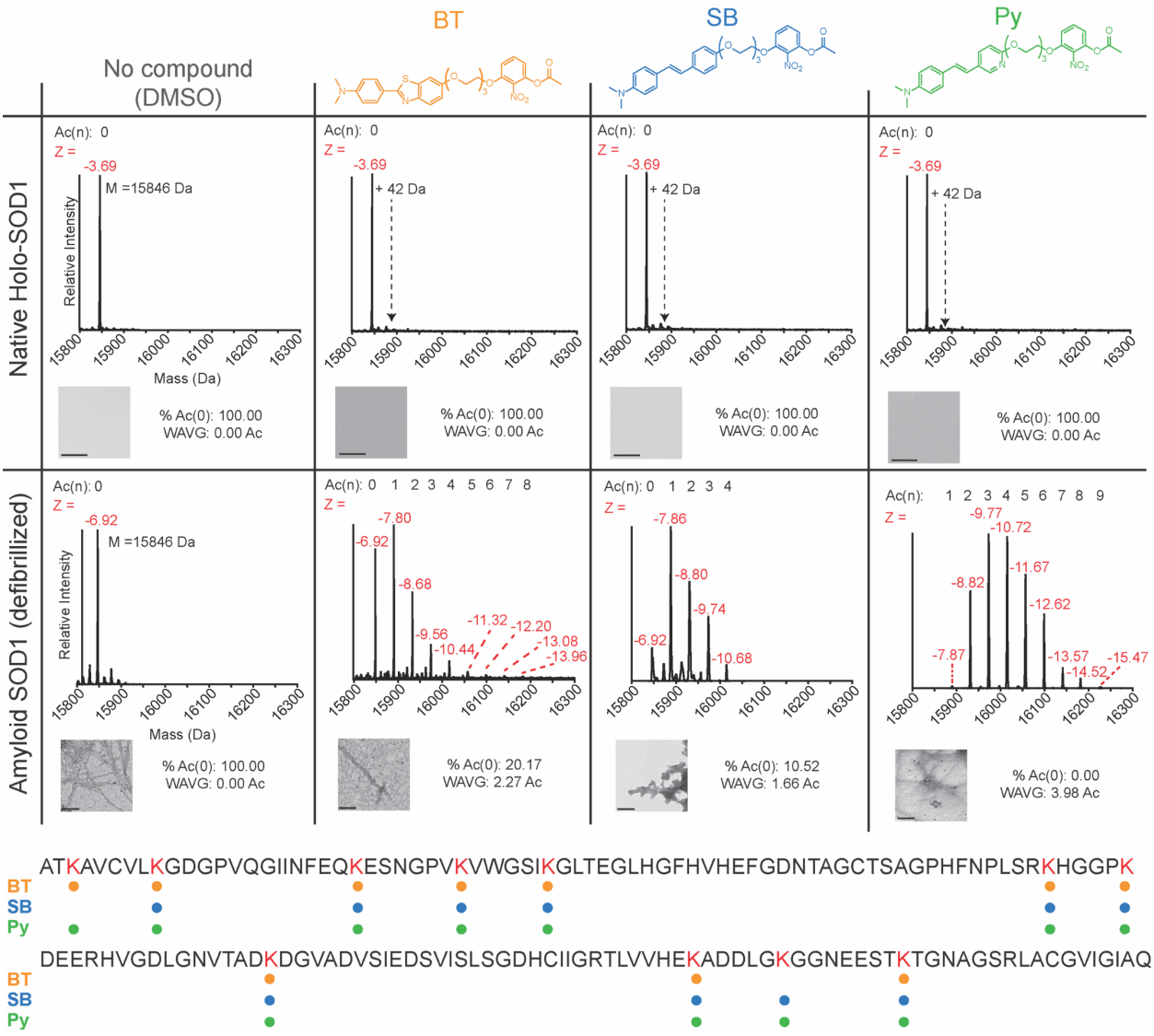

Figure 2. Reactivity grid for acetylation of native or fibrillar WT SOD1 (vertical axis) by BT, SB, or Py molecular maces (horizontal axis). Mass spectra of native WT SOD1 (top) and (defibrillized) amyloid WT SOD1 (bottom) following 5-day incubation with BT, SB, or Py molecular maces. Solutions of fibrillar and native SOD1 were solubilized with HFIP prior to mass spectrometric analysis. The number of acetyl groups per monomer corresponding to each peak is shown as Ac(n) (weighted average (WAVG) number of acetyl modifications per monomer). The amount of protein remaining unacetylated (% Ac(0)) is noted in the bottom right of each panel. In cases where acetylation was not observed (i.e., native WT SOD1 incubated with any of the three molecular maces), the mass at which acetylated SOD1 would have appeared is indicated by "+42 Da". The measured net charge of an SOD1 monomer with the respective number of acetyl modifications is shown in red (determined via capillary electrophoresis). Transmission electron micrographs of fibrillar or native WT SOD1 after reaction with each molecular mace are shown below mass spectra. Scale bars = 100 nm. The SOD1 sequence illustrates residues that were acetylated by molecular maces (•).

10.1002/anie.202103548

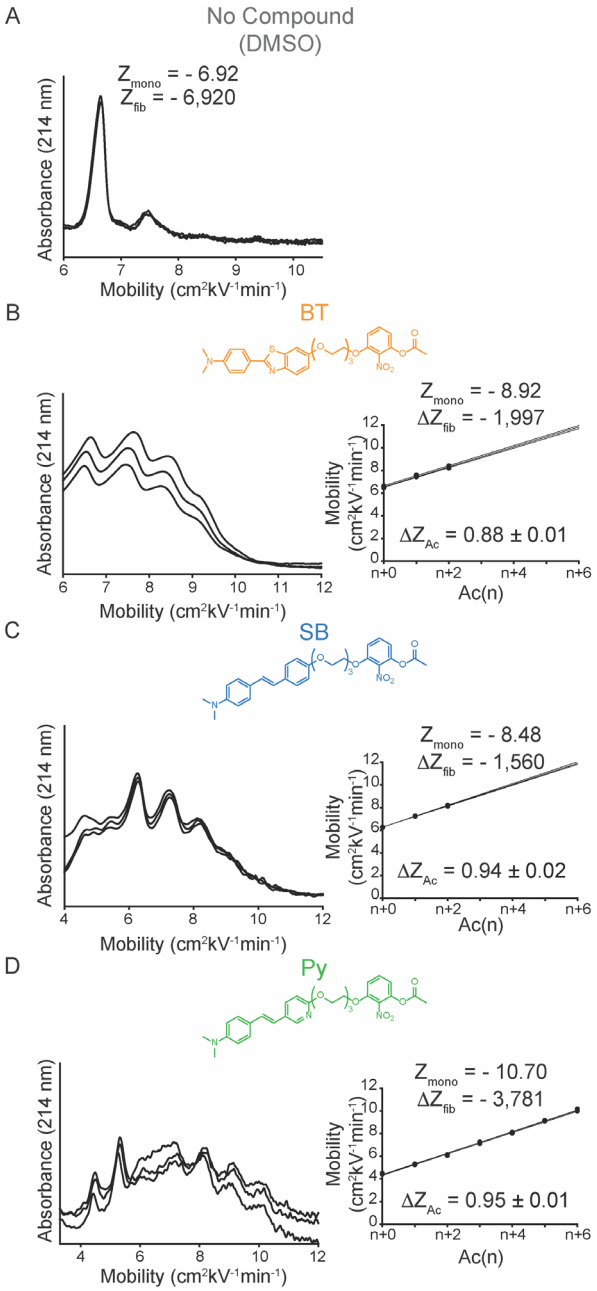

Figure 3. Quantifying effect of lysine acetylation on net charge (*Z*) of fibrillar SOD1 with capillary zone electrophoresis. Capillary electropherograms of defibrillized apo-SOD1 following incubation with (A) DMSO and (B-D) "ball and chain" molecular maces. Linear plots of electrophoretic mobility of SOD1 chain vs. number of acetyl modifications (n) are shown to right of each electropherogram (ΔZ_{Ac} = 0.88-0.95 units per lysine acetylation). The value Z_{mono} refers to the net charge of each SOD1 polypeptide containing the weighted average number of acetylations (inferred from MS). The value ΔZ_{fib} refers to the corresponding increase in *Z* for an aggregate composed of 10^3 SOD1 chains. Capillary electrophoresis was performed in triplicate. Note that the satellite peak in A (at 7.5 mobility units) has been previously assigned as deamidation of N26 to aspartate.[44]

10.1002/anie.202103548

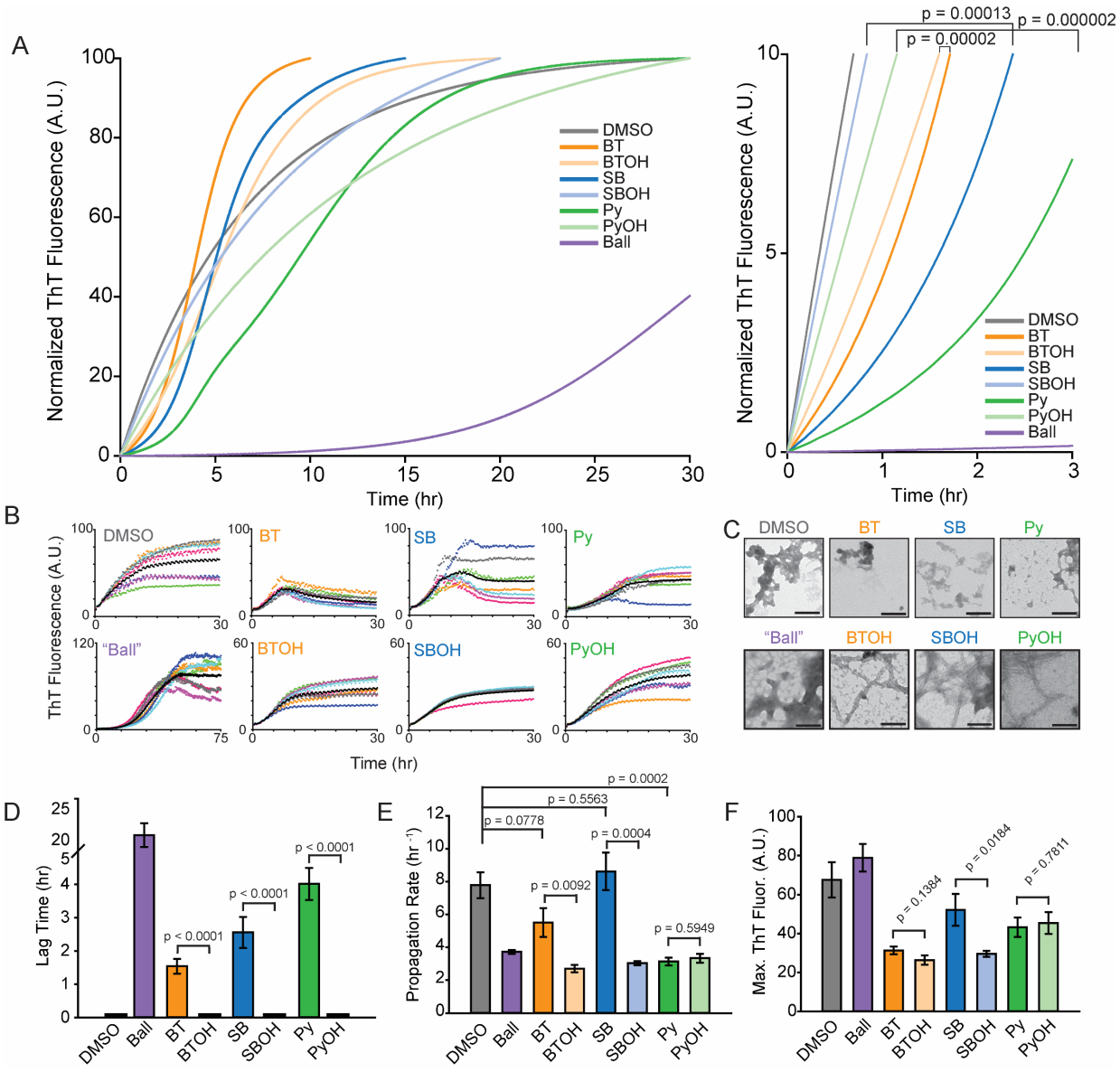

Figure 4. Effect of "ball and chain" maces (BT, SB, Py) and corresponding "whips" (BTOH, SBOH, PyOH) on seeding activity of fibrillar SOD1 *in vitro*. (A) Average, normalized ThT fluorescence of apo WT-SOD1 aggregation seeded by fibrils grown in the presence of "ball and chain" maces, "whips" (lacking aryl ester "ball"), "ball" (lacking handle and chain) and a 3% DMSO control (n = 7 per trace). P values represent comparison of lag time for ball and chain mace and corresponding whip. (B) Raw ThT fluorescence data used to produce (A). Black trace represents the average ThT fluorescence of seven replicate measurements. (C)Transmission electron micrographs of aggregates formed during ThT fluorescence assays; scale bar = 100 nm. (D), Mean lag time, (E) propagation rate, and (F) maximum ThT fluorescence of aggregation assays shown in (A-B). Lag times for DMSO, BTOH, SBOH, and PyOH = 0 as aggregation curve is best fit to an exponential function. Error bars represent the standard error of the mean; p values were calculated using an unpaired Student's t-test.

10.1002/anie.202103548

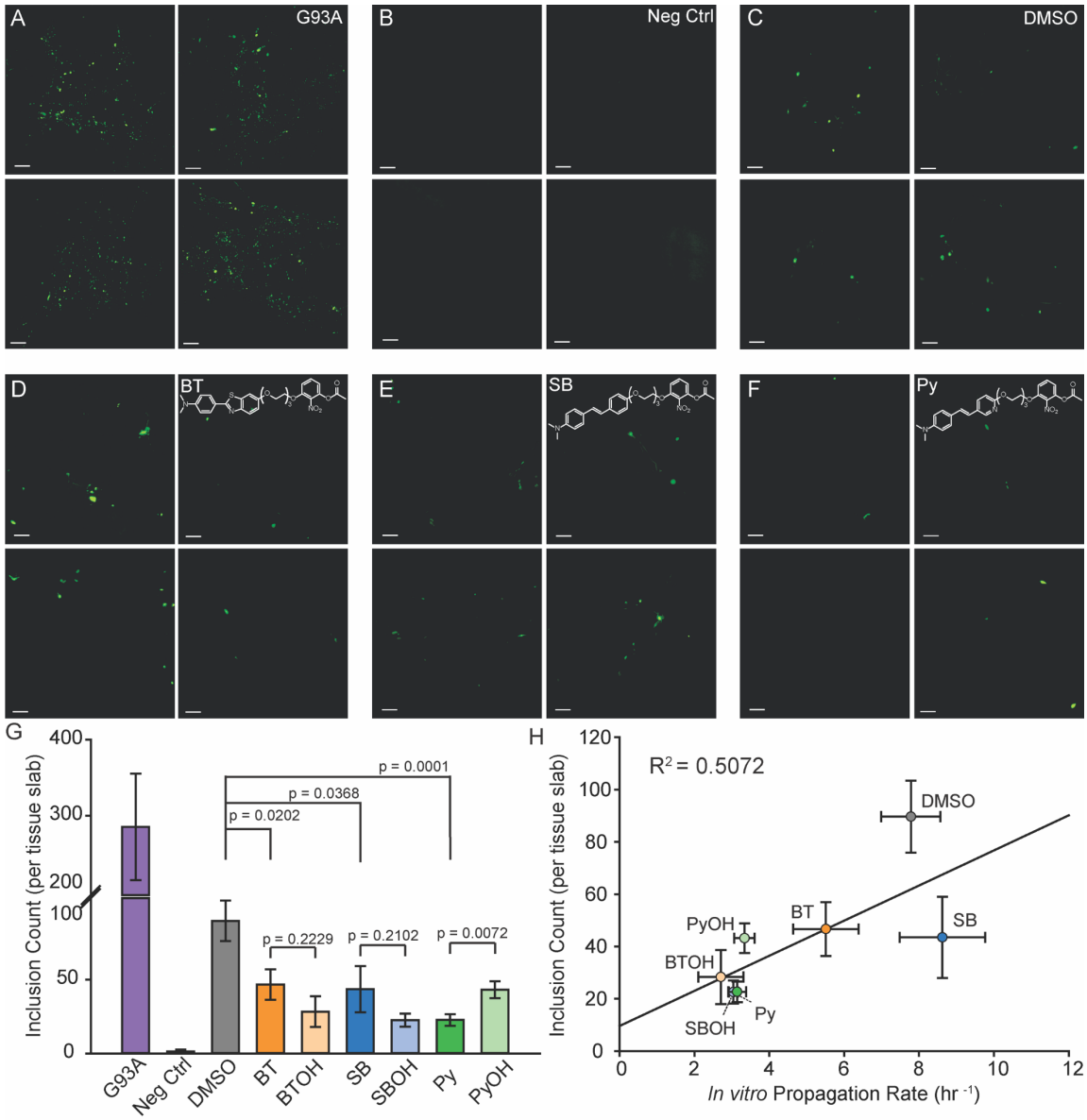

Figure 5. Effect of BT, SB, and Py molecular maces on ability of SOD1 fibrils to induce SOD1 inclusion pathology in organotypic murine spinal cord. Confocal micrographs of cultured G85R-SOD1:YFP spinal cord slab after: (A) addition of spinal cord homogenate of symptomatic G93A-SOD1 mice, (B) no added sample (denoted Neg Ctrl) or (C-F) addition of SOD1 fibrils (formed *in vitro*) that were treated with either DMSO (blank), or BT, SB, Py molecular mace molecules. Scale bars represent 40 µm. Four of 15 biological replicates are shown for each experiment. (G) Average number of inclusions per tissue slab. P values were calculated from an unpaired Student's t-test. (H) Comparison of seeding propensity as measured by *in vitro* propagation rate and *ex vivo* inclusions count. All error bars represent the standard error of the mean. See Supporting Information for additional replicates of each experiment and images of tissue treated with whip analogues. Spinal cords were harvested from non-symptomatic G85R-SOD1:YFP transgenic mice.

References

[1] C. E. Felder, J. Prilusky, I. Silman, J. L. Sussman, *Nucleic Acids Res.* **2007**, *35*, W512-521.

[2] I. Gitlin, J. D. Carbeck, G. M. Whitesides, *Angew. Chem. Int. Ed. Engl.* **2006**, *45*, 3022-3060.

[3] F. Chiti, M. Stefani, N. Taddei, G. Ramponi, C. M. Dobson, *Nature* **2003**, *424*, 805-808.

[4] S. D. Fried, S. Bagchi, S. G. Boxer, *Science* **2014**, *346*, 1510-1514.

[5] M. Y. Tsai, W. Zheng, D. Balamurugan, N. P. Schafer, B. L. Kim, M. S. Cheung, P. G. Wolynes, *Protein Sci.* **2016**, *25*, 255-269.

[6] N. Wiedemar, D. A. Hauser, P. Maser, *Antimicrob. Agents Chemother.* **2020**, *64*.

[7] G. Meisl, T. P. Knowles, D. Klenerman, *Curr. Opin. Neurobiol.* **2020**, *61*, 58-64.

[8] F. Chiti, M. Calamai, N. Taddei, M. Stefani, G. Ramponi, C. M. Dobson, *Proc. Natl. Acad. Sci. U.S.A.* **2002**, *99 Suppl 4*, 16419-16426.

[9] M. S. Lawrence, K. J. Phillips, D. R. Liu, *J. Am. Chem. Soc.* **2007**, *129*, 10110-10112.

[10] E. Sandelin, A. Nordlund, P. M. Andersen, S. S. Marklund, M. Oliveberg, *J. Biol. Chem.* **2007**, *282*, 21230-21236.

[11] B. F. Shaw, H. Arthanari, M. Narovlyansky, A. Durazo, D. P. Frueh, M. P. Pollastri, A. Lee, B. Bilgicer, S. P. Gygi, G. Wagner, G. M. Whitesides, *J. Am. Chem. Soc.* **2010**, *132*, 17411-17425.

[12] B. F. Shaw, G. F. Schneider, B. Bilgicer, G. K. Kaufman, J. M. Neveu, W. S. Lane, J. P. Whitelegge, G. M. Whitesides, *Protein Sci.* **2008**, *17*, 1446-1455.

[13] M. Chattopadhyay, A. Durazo, S. H. Sohn, C. D. Strong, E. B. Gralla, J. P. Whitelegge, J. S. Valentine, *Proc. Natl. Acad. Sci. U.S.A.* **2008**, *105*, 18663-18668.

[14] Y. Shi, R. A. Mowery, B. F. Shaw, *J. Mol. Biol.* **2013**, *425*, 4388-4404.

[15] C. Munch, J. O'Brien, A. Bertolotti, *Proc. Natl. Acad. Sci. U.S.A.* **2011**, *108*, 3548-3553.

[16] J. A. Rodriguez, B. F. Shaw, A. Durazo, S. H. Sohn, P. A. Doucette, A. M. Nersissian, K. F. Faull, D. K. Eggers, A. Tiwari, L. J. Hayward, J. S. Valentine, *Proc. Natl. Acad. Sci. U.S.A.* **2005**, *102*, 10516-10521.

[17] B. G. Trist, J. B. Hilton, D. J. Hare, P. J. Crouch, K. L. Double, *Angew. Chem. Int. Ed. Engl.* **2021**, *60*, 9215-9246.

[18] N. George, E. Gean, A. Nandi, J. R. Brašić, D. F. Wong, in *Imaging of the Human Brain in Health and Disease*, Academic Press, Boston, **2014**, pp. 407-416.

[19] W. Zhang, S. Oya, M. P. Kung, C. Hou, D. L. Maier, H. F. Kung, *J. Med. Chem.* **2005**, *48*, 5980-5988.

[20] W. Zhang, M. P. Kung, S. Oya, C. Hou, H. F. Kung, *Nucl. Med. Biol.* **2007**, *34*, 89-97.

[21] S. Rasouli, A. Abdolvahabi, C. M. Croom, D. L. Plewman, Y. Shi, J. I. Ayers, B. F. Shaw, *J. Biol. Chem.* **2017**, *292*, 19366-19380.

[22] A. Abdolvahabi, Y. Shi, N. R. Rhodes, N. P. Cook, A. A. Marti, B. F. Shaw, *Biophys. J.* **2015**, *108*, 1199-1212.

[23] S. Sinha, D. H. Lopes, Z. Du, E. S. Pang, A. Shanmugam, A. Lomakin, P. Talbiersky, A. Tennstaedt, K. McDaniel, R. Bakshi, P. Y. Kuo, M. Ehrmann, G. B. Benedek, J. A. Loo, F. G. Klarner, T. Schrader, C. Wang, G. Bitan, *J. Am. Chem. Soc.* **2011**, *133*, 16958-16969.

[24] J. Y. Kim, J. W. Lee, Y. S. Kim, Y. Lee, Y. B. Ryu, S. Kim, H. W. Ryu, M. J. Curtis-Long, K. W. Lee, W. S. Lee, K. H. Park, *Chembiochem* **2010**, *11*, 2125-2131.

[25] A. Weichert, A. S. Besemer, M. Liebl, N. Hellmann, I. Koziollek-Drechsler, P. Ip, H. Decker, J. Robertson, A. Chakrabartty, C. Behl, A. M. Clement, *Neruobiol. Dis.* **2014**, *62*, 479-488.
[26] G. Xu, J. I. Ayers, B. L. Roberts, H. Brown, S. Fromholt, C. Green, D. R. Borchelt, *Hum. Mol. Genet.* **2015**, *24*, 1019-1035.
[27] A. Abdolvahabi, Y. Shi, S. Rasouli, C. M. Croom, A. Aliyan, A. A. Marti, B. F. Shaw, *ACS Chem. Neurosci.* **2017**, *8*, 1378-1389.
[28] B. A. Killinger, R. Melki, P. Brundin, J. H. Kordower, *NPJ Parkinson's Dis.* **2019**, *5*.
[29] M. P. Kung, C. Hou, Z. P. Zhuang, D. Skovronsky, H. F. Kung, *Brain Res.* **2004**, *1025*, 98-105.
[30] H. F. Kung, C. W. Lee, Z. P. Zhuang, M. P. Kung, C. Hou, K. Plossl, *J. Am. Chem. Soc.* **2001**, *123*, 12740-12741.
[31] H. Watanabe, M. Ono, T. Ariyoshi, R. Katayanagi, H. Saji, *ACS Chem. Neurosci.* **2017**, *8*, 1656-1662.
[32] J. W. McCabe, C. S. Mallis, K. I. Kocurek, M. L. Poltash, M. Shirzadeh, M. J. Hebert, L. Fan, T. E. Walker, X. Zheng, T. Jiang, S. Dong, C. W. Lin, A. Laganowsky, D. H. Russell, *Anal. Chem.* **2020**, *92*, 11155-11163.
[33] P. Bourassa, C. D. Kanakis, P. Tarantilis, M. G. Pollissiou, H. A. Tajmir-Riahi, *J. Phys. Chem. B* **2010**, *114*, 3348-3354.
[34] P. Sen, S. Fatima, B. Ahmad, R. H. Khan, *Spectrochim. Acta A Mol. Biomol. Spectrosc.* **2009**, *74*, 94-99.
[35] A. Abdolvahabi, Y. Shi, A. Chuprin, S. Rasouli, B. F. Shaw, *ACS Chem. Neurosci.* **2016**, *7*, 799-810.
[36] K. M. Baumer, J. C. Koone, B. F. Shaw, *ACS Chem. Neurosci.* **2020**, *11*, 304-313.
[37] L. Giehm, D. E. Otzen, *Anal. Biochem.* **2010**, *400*, 270-281.
[38] C. Xue, T. Y. Lin, D. Chang, Z. Guo, *R. Soc. Open Sci.* **2017**, *4*, 160696.
[39] J. I. Ayers, J. Diamond, A. Sari, S. Fromholt, A. Galaleldeen, L. W. Ostrow, J. D. Glass, P. J. Hart, D. R. Borchelt, *Acta Neuropathol.* **2016**, *132*, 827-840.
[40] J. I. Ayers, S. Fromholt, M. Koch, A. DeBosier, B. McMahon, G. Xu, D. R. Borchelt, *Acta Neuropathol.* **2014**, *128*, 791-803.
[41] C. M. Grozinger, S. L. Schreiber, *Chem. Biol.* **2002**, *9*, 3-16.
[42] L. M. Needham, J. Weber, J. W. B. Fyfe, O. M. Kabia, D. T. Do, E. Klimont, Y. Zhang, M. Rodrigues, C. M. Dobson, S. Ghandi, S. E. Bohndiek, T. N. Snaddon, S. F. Lee, *R. Soc. Open. Sci.* **2018**, *5*, 171399.
[43] A. W. Pilkington, J. Schupp, M. Nyman, S. J. Valentine, D. M. Smith, J. Legleiter, *ACS Chem. Neurosci.* **2020**, *11*, 146-161.
[44] Y. Shi, N. R. Rhodes, A. Abdolvahabi, T. Kohn, N. P. Cook, A. A. Marti, B. F. Shaw, *J. Am. Chem. Soc.* **2013**, *135*, 15897-15908.

10.1002/anie.202103548

Table of Contents

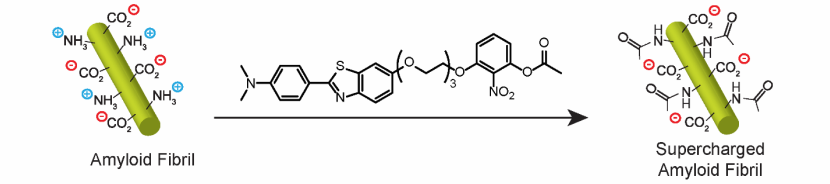

Lead compounds were designed to "supercharge" misfolded forms of proteins linked to amyotrophic lateral sclerosis and Parkinson's disease (i.e., superoxide dismutase-1; α-synuclein). Compounds increased the net negative charge of amyloid fibrils via lysine peracetylation, with minimal to no modification of various proteins in their native state. Supercharged fibrils exhibited weaker seeding activity *in vitro* and in organotypic spinal cord.